Available online at www.sciencedirect.com

SCIENCE DIRECT®

Journal of Organometallic Chemistry 690 (2005) 2736–2744

Journal of Organometallic Chemistry

www.elsevier.com/locate/jorganchem

A new look at the *nido*-undecaborate system

Oleg Volkov [a,1], Krzystof Radacki [b], Rhodri Ll. Thomas [a], Nigam P. Rath [a], Lawrence Barton [a,*]

[a] *Department of Chemistry and Biochemistry and the Center for Molecular Electronics, University of Missouri-St. Louis, St. Louis, MO 63121, USA*
[b] *Institute of Inorganic Chemistry, Bayerische Julius-Maximilians Universität, Würzburg, Germany*

Received 14 September 2004; accepted 7 February 2005
Available online 23 March 2005

Abstract

The structure of the *nido*-undecaborate anion, $[B_{11}H_{14}]^-$, has been re-examined because of what appear to be discrepancies that were observed between our determination of the structure of the anion in $[(Cp_2Zr)_2B_5H_8][B_{11}H_{14}]$ (**1**) and previously published structures. The structure of **1** indicated the presence of two bridging H atoms and another pseudo-bridging one whereas those of a series of published structures indicate the presence of a plane of symmetry with two bridging H atoms and one *endo*-H atom. Thus, we undertook a series of structural determinations and also a computational study at the B3LYP/6-31++G(d,p) level. In addition to **1**, the species studied included $[NBnEt_3][B_{11}H_{14}]$ (**2**), $[NBnEt_3][7\text{-Br-}nido\text{-}B_{11}H_{13}]$ (**3**) and $[NBnEt_3][7\text{-}(\eta^1\text{-dppm})\text{-}nido\text{-}B_{11}H_{12}]$ (**4**). Our structure of **2** indicated the presence of two bridging H atoms and an *endo*-hydrogen atom with some bridging character but that of **3** contained three bridging atoms. As expected the structure of **4** contains two bridging H atoms. Calculations of bond parameters fit well with the experimental data as do the ^{11}B NMR chemical shifts. The latter were calculated for the average of the two open face configurations, one with two bridging and one *endo*-hydrogen and the other with three bridging hydrogen atoms. The difference in energies for these two open face configurations is calculated to be 0.36 kJ/mol, which effectively suggests that the two structures are equally favored.

Keywords: Boron hydrides; Undecaborate; Crystal structures; NMR spectroscopy

1. Introduction

The *nido*-undecaborate anion, $[B_{11}H_{14}]^-$, represents one of the classic structures in polyhedral borane chemistry and it has been known for more than 40 years [1]. It is structurally and electronically related to the series of polyhedral borane and carborane ligands which have found much use as cyclopentadienide analogues in organometallic chemistry [2]. Prior to the first preparation by Muetterties and co-workers [1], Lipscomb and co-workers [3] predicted the structure to be one derived by replacing a BH group in $[B_{12}H_{12}]^{2-}$ by a triangular H_3^+ moiety. This is shown as structure **a** in Fig. 1 which shows possible arrangement of three hydrogen atoms in the open face of the $[B_{11}H_{14}]^-$ cage. The anion is one of a small number of borane species for which the NMR spectra are fluxional at all temperatures and thus the location of the bridging or *endo*-hydrogen atoms is not conclusive from such spectra. Well-defined examples of this are the $[B_9H_{14}]^-$ anion whose structure was recently revised [4], the neutral borane B_5H_{11} [5] and the anion $[B_{11}H_{14}]^-$, the subject of this report. The presence of the H_3^+ moiety in $[B_{11}H_{14}]^-$ has been ascribed as the reason for the lowering the barriers to tautomerism of the *endo*/bridging H atoms [6]. There has been much interest, including some quite recent, in the $[B_{11}H_{14}]^-$ anion and related species from both experimental and

---

[*] Corresponding author. Tel./fax: +1 314 515 5342.
E-mail address: lbarton@umsl.edu (L. Barton).

[1] Permanent address: Institute of Inorganic Chemistry, Russian Academy of Sciences, 630090, Novosibirsk, Russia.

0022-328X/$ - see front matter © 2005 Elsevier B.V. All rights reserved.
doi:10.1016/j.jorganchem.2005.02.029

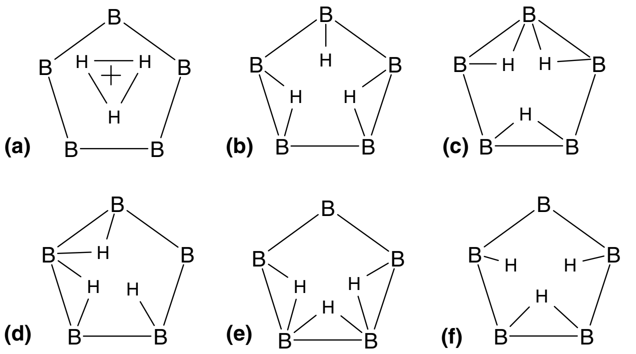

Fig. 1. Some of the possible arrangements of the *endo*/bridging hydrogen atoms in the open face of the $[B_{11}H_{14}]^-$ anion.

theoretical perspectives [7–13]. Recent crystal structure determinations of the anion indicate that there are two bridging-hydrogen atoms and one *endo*-hydrogen in the open face of the cluster, [9a,9b] illustrated as structure **b** in Fig. 1, but calculations suggest that the barrier to interconversion of bridging and *endo*-hydrogen atoms is only 1.4 kcal/mol [10b]. Additionally, a structure of the derivative anion $[7\text{-}t\text{-hexyl-}B_{11}H_{13}]^-$ indicating the presence of three bridging H atoms in the open face was reported [14]. Our recent work on the formation of the novel species $[(Cp_2Zr)_2B_5H_8][B_{11}H_{14}]$ [15], indicated some differences from the observed structure for the anion in this species so we undertook a study of a series of *nido*-undecaborate anion clusters.

2. Experimental

2.1. General

Solvents used were reagent grade and were dried before use. The reactions were carried out using a Schlenk line and standard techniques for handling air-sensitive compounds [16]. $[NBnEt_3][\textit{nido}\text{-}B_{11}H_{14}]$ was prepared from the reaction of $B_{10}H_{14}$ and $NaBH_4$ [1] and $[NBnEt_3]_2[\textit{closo}\text{-}B_{11}H_{11}]$ was prepared as described in [9c]. NMR spectroscopy was carried out on a Bruker ARX 500 spectrometer operating at 500.1 MHz for proton, 160.5 MHz for boron-11, and at 202.5 MHz for phosphorus-31. Chemical shifts are reported in ppm to low field (high frequency) of $Et_2O \cdot BF_3$ for ^{11}B, of $SiMe_4$ for ^1H and of 85% H_3PO_4 for ^{31}P. Elemental analyses were attempted by Atlantic Microlabs, Inc., Norcross, GA. NMR spectra were run on all samples sent for mass spectra and crystal growth was generated from NMR samples, after spectral analysis. The samples were evaporated to dryness and then dissolved in the appropriate solvent for subsequent crystallization. The mass spectra were measured in the FAB mode on a JEOL MStation JMS-700 spectrometer using 3-nitrobenzyl alcohol (3-NBA).

2.2. Reaction of $[NBnEt_3]_2[\textit{closo}\text{-}B_{11}H_{11}]$ with $HgBr_2$

A sample of $[NBnEt_3]_2[\textit{closo}\text{-}B_{11}H_{11}]$ (90 mg, 0.175 mmol) was added under nitrogen to a solution of $HgBr_2$ (63 mg, 0.175 mmol) in 30 mL CH_2Cl_2 and stirred overnight at room temperature. Then the solution was filtered, reduced in volume, and applied to the Chromatotron (a radial chromatograph obtained from Harrison Research, Palo Alto, CA) using a 25 cm diameter circular plate coated with 0.1 cm of silica gel (EM science) and CH_2Cl_2/MeCN (6:1) mixture as the mobile phase. Two components were isolated. The second component was identified as previously reported $[NBnEt_3]_2[B_{22}H_{22}]$ [9c] (8 mg, 0.012 mmol; 14%). The first component after recrystallization in CH_2Cl_2/hexane was identified as $[NBnEt_3][7\text{-Br-}\textit{nido}\text{-}B_{11}H_{13}]$ (**3**) (33 mg, 0.082 mmol; 47%). Single crystals of this compound were obtained by slow diffusion of hexane into CH_2Cl_2 solution. HR-MS for anion $[7\text{-Br-}\textit{nido}\text{-}B_{11}H_{13}]^-$ (FAB with 3-NBA) *m/z* calculated for $H_{13}B_{11}Br$: 212.1285; found: 212.1355. The mass envelopes for the measured masses match quite well with those calculated from the known isotopic abundances of the constituent elements. ^{11}B NMR (CD_2Cl_2, 25 °C, in brackets: B atoms correlated by 2 D-$^{11}B/^{11}B$ COSY): δ −8.1 ($J(H/B) = 147$ Hz, B8/B11 [B2/B3; B4/B6; B7]), −12.3 ($J(H/B) = 146$ Hz, B2/B3 [B1/B5; B4/B6; B7; B8/B11]), −13.6 ($J(H/B) = 143$ Hz, B1/B5 [B2/B3; B4/B6; B9/B10]), −17.0 ($J(H/B) = 155$ Hz, B9/B10 [B1/B5; B4/B6]), −17.6 (s, B7 [B2/B3; B8/B11]), −21.2 ($J(H/B) = 142$ Hz, B4/B6 [B1/B5; B2/B3; B8/B11; B9/B10]). ^1H NMR (CD_2Cl_2, 25 °C): δ 7.59–7.42 (m, 5H; C_6H_5), 4.42 (s, 2H, $CH_2C_6H_5$), 3.24 (q, $J(H,H) = 7$ Hz, 6H, CH_2CH_3), 1.47 (t, $J(H,H) = 7$ Hz, 9H, CH_2CH_3). Additional $^1H\{^{11}B\}$ NMR (CD_2Cl_2, 25 °C, 2D-$^1H/^{11}B$ HMQC): δ 2.37 (H8/H11), 1.95 (H1 or H5), 1.81 (H2/H3), 1.71 (H9/H10, H1 or H5), 1.00 (H4/H6), −2.80 (3 μ-H, correlated to B7, B8/B11, B9/B10).

2.3. Preparation of $[NBnEt_3][7\text{-}(\eta^1\text{-dppm})\text{-}\textit{nido}\text{-}B_{11}H_{12}]$ (4)

Trifluoroacetic acid (29 mg, 0.25 mmol) was added at −78 °C to a suspension of $[NBnEt_3]_2[\textit{closo}\text{-}B_{11}H_{11}]$ (131 mg, 0.25 mmol) in CH_2Cl_2 (ca. 20 mL) under nitrogen. After a clear solution was formed, a sample of dppm (190 mg, 0.51 mmol) was added. The reaction mixture was stirred for 1 h and then slowly brought to room temperature. All volatiles were removed in vacuo. The dry material was recrystallized in CH_2Cl_2/EtOH and CH_2Cl_2/pentane to give a colorless product, identified as $[NBnEt_3][7\text{-}(\eta^1\text{-dppm})\text{-}\textit{nido}\text{-}B_{11}H_{12}]$ (**4**) (161 mg, 0.23 mmol; 92%). Anal. Calc. for $C_{38}H_{56}B_{11}NP_2$: C, 64.49; H, 7.98. Found: C, 64.74; H, 7.95%. HR-MS for anion $[7\text{-}(\eta^1\text{-dppm})\text{-}\textit{nido}\text{-}B_{11}H_{12}]^-$ (VG ZAB-E, FAB with 3-NBA) *m/z* calculated for $C_{25}H_{34}B_{11}P_2$: 515.3246; found: 515.3271. The mass envelopes for the measured masses match quite well with those calculated from the known isotopic abundances of the constituent elements. ^{11}B NMR (CD_2Cl_2, 25 °C): δ −4.8 (d, J(H/B) = 125 Hz, 1B), −12.1 (d, J(H/B) = 131 Hz, 2B), −15.4 (br d, 2B), −18.6 (d, J(P/B) = 110 Hz, 1B), −21.9 (br d, 2B), −27.6 (d, J(H/B) = 140 Hz, 1B), −28.5 (d, J(H/B) = 135 Hz, 2B). ^{1}H NMR (CD_2Cl_2, 25 °C): δ 7.68–7.19 (m, 25H; C_6H_5), 4.28 (s, 2H; $CH_2C_6H_5$), 2.86 (br, 2H; $CH_2P_2Ph_4$), 2.81 (q, J(H/H) = 7 Hz, 6H; CH_2CH_3), 1.39 (t, J(H/H) = 7 Hz, 9H; CH_2CH_3). Additional ^{1}H{^{11}B} NMR (CD_2Cl_2, 25 °C): δ 1.96 (2H, BH), 1.33 (1H, BH), 1.25 (2H, BH), 1.03 (2H, BH), 0.81 (1H, BH), 0.48 (2H, BH), −4.48 (2H, μ-H). ^{31}P{^{1}H} NMR (CD_2Cl_2, 25 °C): δ 11.0 (br d, 1P), −26.5 (d, J(P,P) = 41 Hz, 1P). Single crystals of [$NBnEt_3$][7-(η^1-dppm)-*nido*-$B_{11}H_{12}$] suitable for X-ray analysis, were grown for the phosphines oxide, by slow diffusion of Et_2O into CH_2Cl_2 solution. As noted elsewhere the structure determined was for a sample containing 10% phosphine oxide.

2.4. Calculations

All the calculations reported herein were carried out using the GAUSSIAN-98 package running on a cluster of Linux workstations [17]. Since frequency analyses at the MP2 level were computationally too expensive, calculations were performed using DFT methods, applying the three hybrid functional B3LYP using 6-31G(d,p) and 6-31++G(d,p) basis functions sets [18–20]. The geometry for the molecules with C_s symmetry were defined in internal coordinates and optimized using the Berny algorithm, and the C_1 symmetry transition state was found using the synchronous transit-guided quasi-Newton method (STQN) [21,22]. Vibrational analyses for all stationary points were carried out analytically [23]. The nature of the transition state was confirmed by following the reaction path method (IRC) [24]. NMR spectra were calculated using the GIAO method. Chemical shifts were adjusted to tetramethylsilane and diborane(6) and recalculate to normal – TMS and $BF_3 \cdot Et_2O$ – scales. The total energies E_h and the ZPVE (in parentheses) in hartree, calculated at the 6-31++G(d,p) and 6-31G(d,p) basis set levels, respectively, are as follows: minimum **b** −282.004071 (0.181092) and −281.991616 (0.181827); minimum **c** −282.003933 (0.181003) and −281.991496 (0.181719); transition state **b/c** −282.003503 (0.180352) and −281.991176 (0.181176). The letters **a**, **b** and **c** refer to the labeled structures in Fig. 1.

Table 1
Crystal data and structure refinement for [$NBnEt_3$][$B_{11}H_{14}$] (**2**), [$NBnEt_3$][7-Br-*nido*-$B_{11}H_{13}$] (**3**) and [$NBnEt_3$][7-{η^1-$PPh_2CH_2PPh_2(O)$}-*nido*-$B_{11}H_{12}$] (**4**)

Compound	**2**	**3**	**4**
Empirical formula	$C_{13}H_{36}B_{11}N$	$C_{13}H_{35}B_{11}BrN$	$C_{38}H_{56}B_{11}NO_{0.1}P_2$
Formula weight	325.34	404.24	709.29
T (K)	165(2)	213(2)	165(2)
λ (Å)	0.71073	0.71073	0.71073
Crystal system	Monoclinic	Monoclinic	Monoclinic
Space group	$P2_1/n$	$P2_1/n$	$P2_1/c$
a (Å)	9.2985(2)	9.4919(3)	19.0380(4)
b (Å)	17.6331(3)	18.6245(5)	12.4138(2)
c (Å)	13.2560(3)	12.7629(4)	18.3673(4)
α (°)	90	90	90
β (°)	105.4170(10)	102.314(2)	110.1470(10)
γ (°)	90.	90.	90
V (Å^{-3})	2095.26(7)	2204.34(11)	4075.21
Z	4	4	4
D_{calc} (Mg m^{-3})	1.031	1.218	1.156
Absorption coefficient (mm^{-1})	0.050	1.862	0.136
F(000)	704	840	1507
Crystal size (mm)	0.33 × 0.26 × 0.22	0.34 × 0.30 × 0.18	0.40 × 0.26 × 0.11
θ Range for data collection (°)	1.97–29.00	1.97–28.06	2.00–25.00
Index ranges	$-12 \leqslant h \leqslant 12$, $-24 \leqslant k \leqslant 23$, $-17 \leqslant l \leqslant 18$	$-12 \leqslant h \leqslant 12$, $-24 \leqslant k \leqslant 24$, $-16 \leqslant l \leqslant 16$	$-22 \leqslant h \leqslant 22$, $-14 \leqslant k \leqslant 14$, $-21 \leqslant l \leqslant 21$
Number of reflections collected	43722	40799	38153
Number of independent reflections (R_{int})	5553 (0.041)	5337 (0.061)	7179 (0.063)
Maximum and minimum transmission	0.9890 and 0.9835	0.7304 and 0.5700	0.9852 and 0.9475
Data/restraints/parameters	5553/0/282	5337/0/222	7179/0/526
Goodness-of-fit on F^2	1.028	1.012	1.026
Final R indices [$I > 2\sigma(I)$] R_1	$R_1 = 0.0478$, $wR_2 = 0.1207$	$R_1 = 0.0490$, $wR_2 = 0.1078$	$R_1 = 0.0518$, $wR_2 = 0.1263$
wR_2 (all data)	$R_1 = 0.0801$, $wR_2 = 0.1472$	$R_1 = 0.0803$, $wR_2 = 0.1238$	$R_1 = 0.0823$, $wR_2 = 0.1439$
Largest difference in peak and hole (e Å^{-3})	0.301 and −0.221	0.787 and −0.410	0.520 and −0.237

Table 2
Selected bond distances (Å) and angles (°) for[$NBnEt_3$][$B_{11}H_{14}$] (**2**), [$NBnEt_3$][7-Br-*nido*-$B_{11}H_{13}$] (**3**) and [$NBnEt_3$][7-{η^1-PPh_2CH_2-$PPh_2(O)$}-*nido*-$B_{11}H_{12}$] (**4**)

Compound	**2**	**3**	**4**
Bond distance (Å)			
B(3)–B(7)	1.767(2)	1.769(5)	1.756(4)
B(3)–B(4)	1.778(2)	1.773(5)	1.794(4)
B(3)–B(8)	1.780(2)	1.765(5)	1.803(4)
B(3)–H(3)	1.101(17)	1.08(3)	1.14(3)
B(4)–B(9)	1.773(2)	1.747(6)	1.786(4)
B(4)–B(5)	1.774(2)	1.779(6)	1.783(5)
B(4)–B(8)	1.784(2)	1.746(5)	1.795(5)
B(4)–H(4)	1.093(16)	1.04(4)	1.09(3)
B(5)–B(10)	1.757(2)	1.786(6)	1.769(5)
B(5)–B(9)	1.767(2)	1.772(6)	1.758(5)
B(5)–B(6)	1.782(2)	1.775(6)	1.769(5)
B(5)–H(5)	1.104(16)	1.08(3)	1.09(3)
B(6)–B(10)	1.772(2)	1.783(6)	1.786(5)
B(6)–B(11)	1.779(2)	1.758(5)	1.792(5)
B(6)–H(6)	1.132(17)	1.10(3)	1.08(3)
B(7)–B(11)	1.890(2)	1.902(5)	1.753(4)
B(7)–B(8)	1.902(2)	1.873(5)	1.772(4)
B(7)–H(7)	1.070(17)		
B(7)–H(7-*endo*)	1.29(3)		
B(7)–H(78)		1.26(4)	
B(8)–B(9)	1.885(2)	1.909(6)	1.886(4)
B(8)–H(8)	1.071(17)	1.03(3)	1.09(3)
B(8)–H(89)	1.41(3)	1.26(4)	1.27(3)
B(9)–B(10)	1.919(2)	1.898(6)	1.855(5)
B(9)–H(9)	1.117(17)	1.07(4)	1.06(3)
B(9)–H(89)	1.22(3)		1.22(3)
B(9)–H(910)		1.04(5)	
B(10)–H(910)		1.49(5)	
B(10)–B(11)	1.874(2)	1.900(5)	1.894(4)
B(10)–H(10)	1.142(18)	1.06(3)	1.13(3)
B(10)–H(101)	1.34(3)	1.51(4)	1.36(3)
B(11)–H(11)	1.101(16)	1.06(3)	1.09(3)
B(11)–H(101)	1.31(3)	1.13(4)	1.32(3)
Bond angle (°)			
B(7)–B(8)–B(9)	108.64(11)	108.0(2)	109.3(2)
B(8)–B(9)–B(10)	107.27(11)	106.4(2)	105.6(2)
B(9)–B(10)–B(11)	107.87(11)	110.1(3)	105.9(2)
B(10)–B(11)–B(7)	108.92(11)	105.4(2)	109.2(2)
B(11)–B(7)–B(8)	107.28(10)	110.0(2)	109.8(2)

2.5. X-ray structure determinations

Single crystals with appropriate dimensions were mounted on glass fibers in random orientation. Preliminary examination and data collection were performed using a Bruker SMART Charge Coupled Device (CCD) Detector single crystal X-ray diffractometer using graphite monochromated Mo Kα radiation ($\lambda = 0.71073$ Å) equipped with a sealed tube X-ray source. Preliminary unit cell constants were determined with a set of 45 narrow frames (0.3 in ϖ) scans. Data sets typically consisted of 3636 frames of intensity data collected with a frame width of 0.3 in ϖ and counting time of 15–30 s/frame at a crystal to detector distance of 4.950 cm. The double pass method of scanning was used to exclude any noise. The collected frames were integrated using an orientation matrix determined from the narrow frame scans. SMART and SAINT software packages [25] were used for data collection and data integration, respectively. Analysis of the integrated data did not show any decay. Final cell constants were determined by global refinement of the *xyz* centroids of thresholded reflections from the complete data set. Collected data were corrected for systematic errors using SADABS [26] based on the Laue symmetry using equivalent reflections. Crystal data and intensity data collection parameters are listed in Table 1. Structure solutions and refinement were carried out using the SHELXTL-PLUS software package [27]. The structures were solved by direct methods and refined successfully in the monoclinic space groups $P2_1/n$ for **2** and **3** and $P2_1/c$ for **4**. Full-matrix least-squares refinement was carried out by minimizing $\sum w(F_o^2 - F_c^2)^2$. The non-hydrogen atoms were refined anisotropically to convergence. The cage H's were located in all cases and refined freely. All other hydrogen atoms were treated using appropriate riding models (AFIX m3). Compound **4** crystallizes with ca. 10% phosphines oxide, although elemental analysis of the initially formed compound indicated high purity. The final structure refinement parameters are listed in Table 1 for **2**, **3** and **4**. Complete listings of positional and isotropic displacement coefficients for hydrogen atoms, anisotropic displacement coefficients for the non-hydrogen atoms are deposited as supplementary material. Tables of calculated and observed structure factors are available in electronic format. Selected bond distances and angles are found in Table 2 and the structures of the anions in **2**, **3** and **4** are given in Figs. 3, 4 and 6, respectively.

3. Results and discussion

Our determination of the structure of [$(Cp_2Zr)_2B_5H_8$][$B_{11}H_{14}$] (**1**) identified the undecaborate anion by NMR spectroscopy, X-ray diffraction and other analytical methods as an icosahedron of BH units with one vertex removed. This confirmed the findings of Shore and co-workers [8a] and McGrath and Welch [8b] who identified this cluster as a *nido*-eleven vertex system with three non-*exo*-hydrogen atoms in the open face. However, their results suggested a C_s structure with a pair of B–H–B bridges and a normal *endo*-hydrogen atom, illustrated as structure **b** in Fig. 1. Since not all the cage hydrogen atoms were located in our study, we are unable to confirm this finding, although our data for **1** suggested that there were two adjacent B–H–B moieties and a non-adjacent very asymmetric *endo*-H atom affording a structure of C_1 symmetry (see Fig. 2). The best description is a combination of structures **d** and **c**, both of which are illustrated in Fig. 1, rather than the C_s configuration observed in [8a,8b]. In the structure

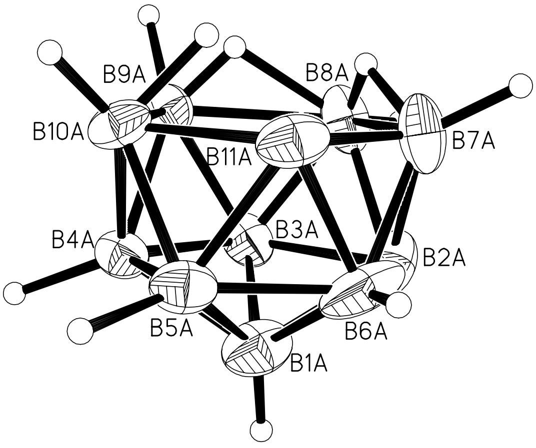

Fig. 2. Crystallographically determined molecular structure for the [*nido*-$B_{11}H_{14}$] anion in [$(Cp_2Zr)_2B_5H_8$][$B_{11}H_{14}$] (**1**), drawn with 15% probability ellipsoids [15].

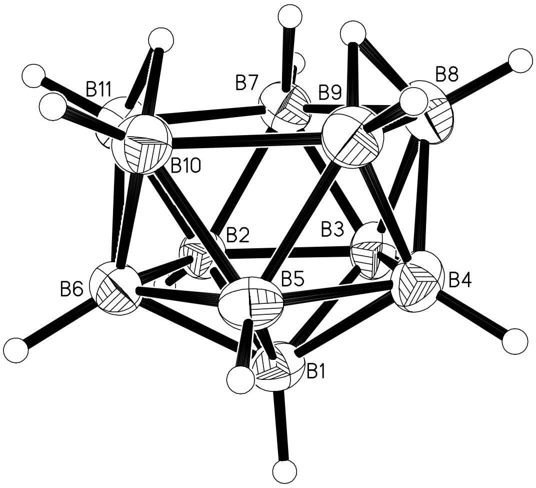

Fig. 3. Crystallographically determined molecular structure for the [*nido*-$B_{11}H_{14}$] anion in [$NBnEt_3$][*nido*-$B_{11}H_{14}$] (**2**) drawn with 50% probability ellipsoids.

determination described in [8b] the C_s configuration could be imposed by the crystallographic symmetry since the anion lies on a crystallographic mirror plane. We observed the three hydrogen atoms within the open face of the cluster as a single resonance in the NMR spectra, as did Shore and co-workers [9a], but our structure determination was unable to distinguish completely the bridging-H atoms from the *endo*-terminal H atoms in the open face of the anion. The structure determination for **1**, however, did not locate all the hydrogen atoms in the open face so there are more serious problems with the structure but it was this structure determination that stimulated our interest in studying further this unresolved structural problem.

Thus, to resolve this apparently discrepancy, we attempted to grow crystals, suitable for X-ray analysis, of $[B_{11}H_{14}]^-$ salts using a series of counter ions including $[N(PPh_3)_2]^+$($[PPN^+]$), $[NBnEt_3]^+$ and $[(\eta^5\text{-}C_5H_5)Fe(\eta^5\text{-}C_5H_4CH_2(Me)_3N)]^+$. Good crystals were difficult to obtain and structures of varying quality were obtained. The most successful was with the $[NBnEt_3]^+$ cation. The structure obtained shows two bridging H atoms with a third *endo*-hydrogen which is clearly not on a plane in the molecule and must have some bridging character, as indicated in Fig. 3. The H atoms from the boron cages were located and refined and an examination of the geometrical parameters indicates that the unique *endo*-H atom in the open face is very asymmetric. For example, the distances of the *endo*-hydrogen H(78) from the adjacent B atoms are quite different, B(8)–H(78) is 1.68(3) Å and B(11)–H(78) is 1.99(3) Å. Also the angle between the planes H(78)–B(7)–B(1) and B(7)–B(1)–B(5) is 9.1(6)°. This would be zero if H(78) fell on a plane of symmetry. Actually the planes B(7)–B(1)–B(5) and B(5)–B(1)–H(1) fall at 1.6(18)° to each other, suggesting that the *exo*-H(1) atom is not on a plane of symmetry, but the difference between this and the value 9.1(6)°, for the *endo*-H atom plane implies statistical significance to our assertion. Thus, there is no plane of symmetry in the ion and this is confirmed from an examination of the bond distances and angles shown in Table 2 and also in Fig. 7 which shows comparative bond distances for species **1**–**4**. Indeed the structure resembles that determined by Shore and co-workers [8a] with some subtle differences. For example that report shows the B-(*endo*-H) distance as 1.13 Å and we report 1.29(3) Å, which may be statistically significant.

A serendipitous discovery involved the product of the reaction between $[NBnEt_3]_2$[*closo*-$B_{11}H_{11}$] with $HgBr_2$. We have recently reported some results of attempts to couple the anion $[B_{22}H_{22}]^{2-}$ to form larger macropolyhedral boranes from the reaction between $[NBnEt_3]_2[B_{22}H_{22}]$ and $HgBr_2$ but the products were salts of the $[B_{22}H_{21}OH]^{2-}$ and $[B_{22}H_{21}OEt]^{2-}$ anions [28]. Related chemistry involving attempts to couple $[B_{11}H_{11}]^{2-}$ to afford $[B_{22}H_{22}]^{2-}$ in larger yield led to the formation of [$NBnEt_3$][7-Br-*nido*-$B_{11}H_{13}$] (**3**) as the major product with the $[B_{22}H_{22}]^{2-}$ salt as the minor one. The formulation was indicated by negative ion high resolution mass spectrometry, by NMR spectra and a crystal structure determination confirmed it. Again, as indicated in Fig. 4, the structure appears to deviate from the expected structure **b** in Fig. 1 and resembles structure **c**. Thus, there are three bridging H atoms in the open face of the cage. As seen in Fig. 7, there is no apparent correlation between the bond distances and the presence of bridging H atoms; a point mentioned below. The cage hydrogen atoms were located and refined in this structure determination. It is of interest to examine the location of the bridging H atoms. H(78) is symmetrical within error limits but the other two are not. The B–Hμ distances for H(910) are 1.04(5) and 1.49(5)

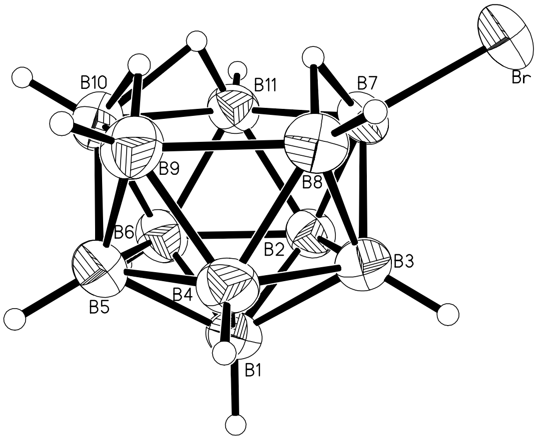

Fig. 4. Crystallographically determined molecular structure for the [7-Br-*nido*-$B_{11}H_{13}$] anion in [$NBnEt_3$][7-Br-*nido*-$B_{11}H_{13}$] (**3**) drawn with 50% probability ellipsoids.

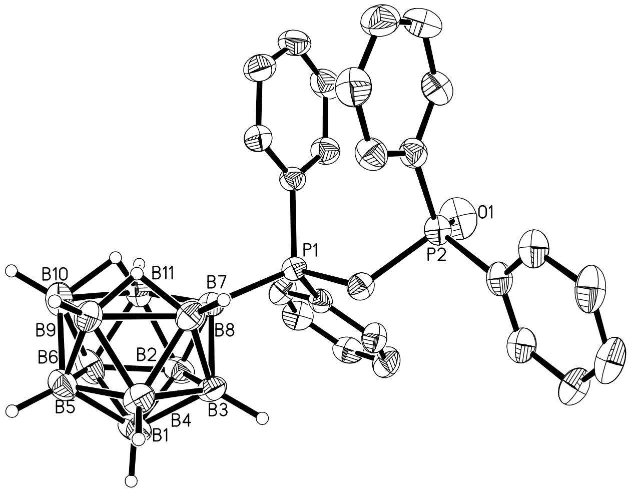

Fig. 6. Crystallographically determined molecular structure for the [7-{η^1-$PPh_2CH_2PPh_2(O)$}-*nido*-$B_{11}H_{12}$] anion in [$NBnEt_3$][7-{η^1-$PPh_2CH_2PPh_2(O)$}-*nido*-$B_{11}H_{12}$] (**4**) drawn with 50% probability ellipsoids.

and for H(101) they are 1.13(4) and 1.51(4) Å. Thus, one of the Hμ atoms seems quite normal and the other two seem to have *endo*-H character, seemingly rendering the structure of **3** to be a combination of structures **c** and **f** in Fig. 1. It is useful to compare the structure of **3** with that of the 7-*t*-hexyl-[$B_{11}H_{13}$]$^-$ (**5**) anion [14]. In the latter, the substituent *t*-hexyl moiety sits adjacent to two bridging H atoms and thus on a pseudo plane of symmetry but in **3** the Br substituent is disposed asymmetrically adjacent to the unique bridging H atom, as illustrated in Fig. 5. In both cases the substituent imparts some cage distortion.

The next step was to impose a plane of symmetry on the cage by preparing [$NBnEt_3$][7-(η^1-dppm)-nido-$B_{11}H_{12}$] (**4**) by protonation of [$NBnEt_3$]$_2$[*closo*-$B_{11}H_{11}$] followed by treatment with dppm. The product **4**, a new compound, was obtained pure, essentially in quantitative yield. Crystals suitable for X-ray analysis were grown and the structure is given in Fig. 6. During crystallization, some oxidation occurs and the species for which crystals were obtained contains ca. 10% phosphines oxide, and the O atom is seen in the figure. In this case, the cage is symmetrical with a plane of symmetry and it resembles structure **b** without the extra *endo*-hydrogen atom. In this system the non-bridged B–B distances, as expected, are shorter than the bridged ones as is seen for the classic system B_6H_{10}. In B_6H_{10}, the non-bridged B–B distance is very short, at 1.626 Å, whereas the bridged distances are 1.741 and 1.789 Å [29]. This feature is not consistently observed for the series of compounds **1**–**4** as seen in Fig. 7.

To further probe this system, calculations at the B3LYP/6-31++G(d,p) level were undertaken. To locate

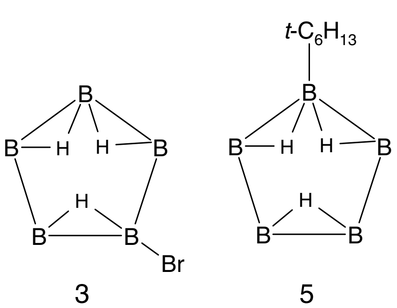

Fig. 5. Comparison of the structures of the anions [7-Br-*nido*-$B_{11}H_{13}$] (**3**) and [7-*t*-C_6H_{13}-*nido*-$B_{11}H_{13}$] (**5**) [14].

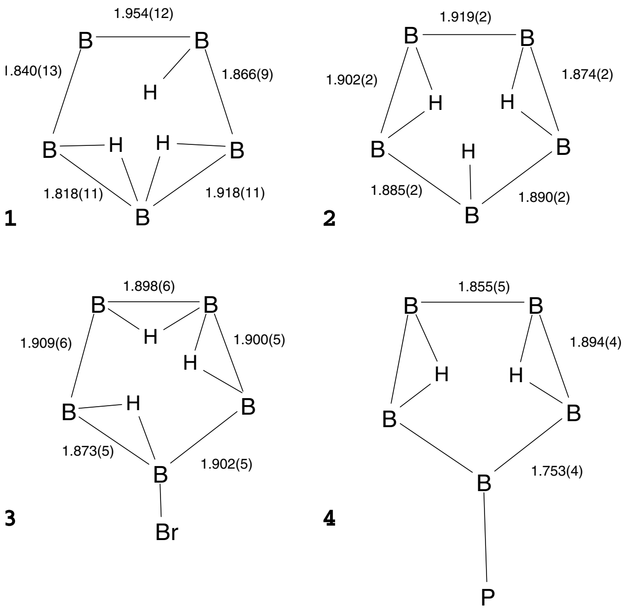

Fig. 7. Schematic showing selected bond distances in compounds **1**–**4**. Data for **1** were taken from [15].

stationary points two types of inputs were prepared: one with a bridging hydrogen lying on the plane of symmetry and the second with an *endo*-H atom on it. The positions of the remaining two hydrogen atoms were set at different distances from adjacent boron atoms giving *endo*- or bridging hydrogens. All of these geometries converged to the same two structures; one with one *endo*-hydrogen and two bridging hydrogens (**b** in Fig. 1), and the second with three bridging hydrogens on the open face (**c** in Fig. 1). In the latter two of the bridging H atoms are very asymmetric; affording a structure half-way between **c** and **f**. We choose to refer to this structure as **c** for convenience. The frequency analysis demonstrated that both structures are minima on the potential energy surface, with **c** having an energy value of 0.36 kJ/mol higher than **b**. The calculated transition state for the interconversion of structures **b** and **c** is only 1.49 kJ/mol less favorable than the lower minimum, and this clearly explains the single peak observed in the ^{1}H NMR spectrum for all the H in the open face of this *nido*-cluster. This result is in contrast to previously reported computations at the Hartree–Fock level, where the geometry with three bridging H atoms was found to be the transition state between two **b**-type structures [10b]. The calculated and experimental cage B–B distances are given in Table 3 and computed B–H bonds are given in Fig. 8. As illustrated in this figure, one can visualize the **b**/**c** conversion as a rotation of the H_3-moiety around the C_5 axis of the pentagonal face, or rather, since the overlap populations between the *endo*-hydrogens are close to zero, a synchronous movement of all three hydrogen atoms. The optimized geometric parameters were used as a basis for calculation of chemical shifts and their mean values are in good

Table 3
Calculated and observed bond distances for the $[nido\text{-}B_{11}H_{14}]^{-}$ anion

Bonds in C_s symmetry	Calc. (Å)[a]	Bond	Obs. (Å)[b]	Bond	Obs. (Å)[b]
(B7–B8) = (B7–B11)	1.902	(B7–B8)	1.902(2)	(B7–B11)	1.890(2)
(B7–B3) = (B7–B2)	1.803	(B7–B3)	1.767(2)	(B7B2)	1.759(2)
(B8–B9) = (B11–B10)	1.927	(B8–B9)	1.885(2)	(B10–B11)	1.874(2)
(B8–B3) = (B11–B2)	1.775	(B8–B3)	1.780(2)	(B11–B2)	1.762(2)
(B8–B4) = (B11–B6)	1.760	(B8–B4)	1.784(2)	(B11–B6)	1.779(2)
(B9–B4) = (B10–B6)	1.752	(B4–B9)	1.773(2)	(B6–B10)	1.772(2)
(B9–B5) = (B10–B5)	1.778	(B5–B9)	1.767(2)	(B5B10)	1.757(2)
(B3–B4) = (B2–B6)	1.788	(B3–B4)	1.778(2)	(B2–B6)	1.776(2)
(B3–B2)	1.786	(B2–B3)	1.780(2)		
(B4–B5) = (B5–B6)	1.777	(B4–B5)	1.774(2)	(B5–B6)	1.782(2)
(B5–B1)	1.803	(B1–B5)	1.767(2)		
(B4–B1) = (B6–B1)	1.769	(B1–B4)	1.772(2)	(B1–B6)	1.781(2)
(B3–B1) = (B2–B11)	1.773	(B1–B3)	1.771(2)	(B1–B2)	1.768(2)

[a] Values calculated for structure **c** in Fig. 1.

[b] Observed for structure **2**.

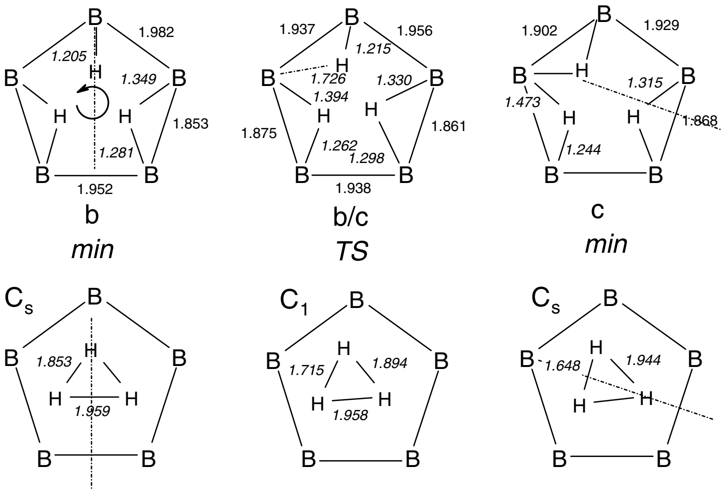

Fig. 8. Schematic showing the computed distances for the minima and the transition state for the favored configurations for the open face of the $[B_{11}H_{14}]^{-}$ anion. Roman numerals indicate B–B distances and the Italics indicate B–H distances.

Table 4
Observed and calculated ^{11}B NMR chemical shifts[a]

Atoms	**2** (obs.)[b]	Mean[c]	**b** (calc.)[d]	**c** (calc.)[e]
B(1)	−12.5	−13.1	−9.2	−17.1
B(2–6)	−14.1[a]	−16.6	−16.6	−16.7
B(7–11)	−14.9[a]	−15.2	−12.6	−17.8

[a] In ppm.
[b] Observed spectrum of compound **2**.
[c] The mean of columns 4 and 5.
[d] Calculated for structure **b** in Fig. 1.
[e] Calculated for structure **c** in Fig. 1.

agreement with the observed signals [30] as illustrated in Table 4.

4. Conclusions

The structure of the $[B_{11}H_{14}]^-$ anion has been studied both crystallographically and computationally. The results indicate that the "correct" structure cannot be identified, within the limits of experimental error, and that a true description of the species is that the two structures with a plane of symmetry, one along a B–H-*endo* bond in a system containing two bridging H atoms and one with the plane of symmetry bisecting one of three B–H–B bridging moieties cannot be distinguished. The transition state for the inteconversion between the two is very accessible (1.49 kJ/mol higher in energy than the two minima) and the process involving exchange between the two structures is perhaps best described by a synchronous rotation of the three hydrogen atoms in the open face of the cluster effectively confirming the predictions of William N. Lipscomb 40 years ago.

5. Supplementary material

Crystallographic data (excluding structure factors) for the structures reported in this paper have been deposited with the Cambridge Crystallographic Data Centre: compounds **2**, **3** and **4**. Copies of the information may be obtained free of charge from The Director, CCDC, 12 Union Road, Cambridge CB2 1EZ, UK (fax: +44 1223 336033; e-mail deposit@ccdc.cam.ac.uk).

Acknowledgements

We acknowledge the NSF (Grant No. CHE-9727570), the Missouri Research Board and UM-St. Louis for research grants to L.B. and the NSF and the UM-St. Louis Center for Molecular Electronics and the Missouri Research Board for funds which helped purchase the XRD, NMR, and MS facilities. We also thank Dr. R.E.K. Winter and Mr. Joe Kramer for the MS measurements.

References

[1] V.D. Aftandilian, H.C. Miller, G.W. Parshall, E.L. Muetterties, Inorg. Chem. 1 (1962) 734.
[2] (a) P.A. Wegner, M.F. Hawthorne, Chem. Commun. (1966) 861;
(b) L.F. Warren, M.F. Hawthorne, J. Am. Chem. Soc. 89 (1967) 470;
(c) M.F. Hawthorne, D.C. Young, T.D. Andrews, D.V. Howe, R.L. Pilling, D.A. Pitts, M. Reintjes, L.F. Warren, P.A. Wegner, J. Am. Chem. Soc. 90 (1968) 879.
[3] (a) E.B. Moore, L.L. Lohr, W.N. Lipscomb, J. Chem. Phys. 35 (1961) 1329;
(b) W.N. Lipscomb, in: Boron Hydrides, W.A. Benjamin, New York, 1963, pp. 115–116.
[4] J. Bould, R. Greatrex, J.D. Kennedy, D. Ormsby, M. Londesborough, K.L.F. Callaghan, M. Thornton-Pett, T.R. Spalding, S.J. Teat, W. Clegg, H. Fang, N.P. Rath, L. Barton, J. Am. Chem. Soc. 124 (2002) 7429.
[5] (a) J.B. Leach, T.P. Onak, J. Am. Chem. Soc. 92 (1970) 3513;
(b) J.B. Leach, T.P. Onak, J. Spielman, R.R. Rietz, R. Schaeffer, L.G. Sneddon, Inorg. Chem. 9 (1970) 2170;
(c) R.R. Rietz, R. Schaeffer, L.G. Sneddon, J. Am. Chem. Soc. 92 (1970) 3414.
[6] C.J. Fritchie, Inorg. Chem. 6 (1967) 1199.
[7] (a) G.B. Dunks, K. Palmer-Ordonez, J. Am. Chem. Soc. 100 (1978) 2555;
(b) G.B. Dunks, K. Barker, E. Hedaya, C. Hefner, K. Palmer-Ordonez, P. Remec, Inorg. Chem. 20 (1981) 1692.
[8] (a) T.D. Getman, J.A. Krause, S.G. Shore, Inorg. Chem. 27 (1988) 2398;
(b) T.D. McGrath, A.J. Welch, Acta Crystallogr., Sect. C 53 (1997) 229;
(c) M. Matthias, U. Englert, P. Paetzold, Inorg. Chem. 34 (1995) 5925.
[9] (a) T.D. Getman, H.B. Deng, L.Y. Hsu, S.G. Shore, Inorg. Chem. 28 (1989) 28;
(b) D.L. Keller, J.G. Kester, J.C. Huffman, L.J. Todd, Inorg. Chem. 32 (1993) 5067;
(c) O. Volkov, W. Dirk, U. Englert, P. Paetzold, Z. Anorg. Allg. Chem. 625 (1999) 1193;
(d) W. Dirk, P. Paetzold, K. Radacki, Z. Anorg. Allg. Chem. 627 (2001) 2615.
[10] (a) M. Luo, G. Jiao, Q. Chen, G. Zhou, Wuhan Daxue Xuebao Ziran Kexueban 2 (1986) 95, CA 106, 182852;
(b) P. Maitre, O. Eisenstein, D. Michos, X.-L. Lu, A.R. Siedle, L. Wisnieski, K.W. Zilm, R.H. Crabtree, J. Am. Chem. Soc. 115 (1993) 7747;
(c) A. Es-sofi, C. Serrar, A. Boutalib, A. Ouassas, Theochem 423 (1998) 161.
[11] O. Volkov, P. Paetzold, J. Organomet. Chem. 680 (2003) 301.
[12] (a) S. Körbe, D.B. Sowers, A. Franken, J. Michl, Inorg. Chem. 43 (2004) 8158;
(b) L.A. Gavrilova, L.V. Titov, P.V. Petrovskii, Russ. J. Coord. Chem. 30 (2004) 307.
[13] F.A. Kiani, M. Hofmann, Inorg. Chem. 43 (2004) 8561.
[14] D.F. Gaines, A.N. Bridges, R.K. Hayashi, Inorg. Chem. 33 (1994) 1243.
[15] R.Ll. Thomas, N.P. Rath, L. Barton, Inorg. Chem. 41 (2002) 67.
[16] D.F. Shriver, M.A. Drezdon, The Manipulation of Air-sensitive Compounds, Wiley, New York, 1986.

[17] M.J. Frisch, G.W. Trucks, H.B. Schlegel, G.E. Scuseria, M.A. Robb, J.R. Cheeseman, V.G. Zakrzewski, J.A. Montgomery Jr., R.E. Stratmann, J.C. Burant, S. Dapprich, J.M. Millam, A.D. Daniels, K.N. Kudin, M.C. Strain, O. Farkas, J. Tomasi, V. Barone, M. Cossi, R. Cammi, B. Mennucci, C. Pomelli, C. Adamo, S. Clifford, J. Ochterski, G.A. Petersson, P.Y. Ayala, Q. Cui, K. Morokuma, P. Salvador, J.J. Dannenberg, D.K. Malick, A.D. Rabuck, K. Raghavachari, J.B. Foresman, J. Cioslowski, J.V. Ortiz, A.G. Baboul, B.B. Stefanov, G. Liu, A. Liashenko, P. Piskorz, I. Komaromi, R. Gomperts, R.L. Martin, D.J. Fox, T. Keith, M.A. Al-Laham, C.Y. Peng, A. Nanayakkara, M. Challacombe, P.M.W. Gill, B. Johnson, W. Chen, M.W. Wong, J.L. Andres, C. Gonzalez, M. Head-Gordon, E.S. Replogle, J.A. Pople, GAUSSIAN-98, Revision A 11, Gaussian, Inc., Pittsburgh, PA, 2001.

[18] A.D. Becke, J. Chem. Phys. 98 (1993) 5648.

[19] S.H. Vosko, L. Wilk, M. Nusair, Can. J. Phys. 58 (1980) 1200.

[20] C. Lee, W. Yang, R.G. Parr, Phys. Rev. B 37 (1988) 785.

[21] H.B. Schlegel, J. Comput. Chem. 3 (1982) 214.

[22] C. Peng, P.Y. Ayala, H.B. Schlegel, M.J. Frisch, J. Comput. Chem. 17 (1996) 49.

[23] R.E. Stratmann, J.C. Burant, G.E. Scuseria, M.J. Frisch, J. Chem. Phys. 106 (1997) 10175.

[24] C. Gonzalez, H.B. Schlegel, J. Phys. Chem. 94 (1990) 5523.

[25] Brucker Analytical X-ray, Madison, WI, 2001.

[26] G.M. Sheldrick, University of Goettingen, 2000.

[27] G.M. Sheldrick, Bruker Analytical X-ray Division, Madison, WI, 2001.

[28] O. Volkov, N.P. Rath, L. Barton, J. Organomet. Chem. 608 (2003) 212.

[29] (a) J.C. Huffman, Ph.D. Thesis, Indiana University, 1974;
(b) L. Barton, T.P. Onak, S.G. Shore, Gmelin Handbook of Inorganic Chemistry, Boron Compounds 20New Supplement Series, vol. 54, Springer, Berlin, 1979, pp. 52–79.

[30] N.S. Hosmane, J.R. Wermer, Z. Hong, T.D. Getman, S.G. Shore, Inorg. Chem. 26 (1987) 3638.